J. Physiol. (1952) 116, 424–448

MEASUREMENT OF CURRENT-VOLTAGE RELATIONS IN THE MEMBRANE OF THE GIANT AXON OF *LOLIGO*

BY A. L. HODGKIN, A. F. HUXLEY AND B. KATZ

From the Laboratory of the Marine Biological Association, Plymouth, and the Physiological Laboratory, University of Cambridge

(*Received* 24 *October* 1951)

The importance of ionic movements in excitable tissues has been emphasized by a number of recent experiments. On the one hand, there is the finding that the nervous impulse is associated with an inflow of sodium and an outflow of potassium (e.g. Rothenberg, 1950; Keynes & Lewis, 1951). On the other, there are experiments which show that the rate of rise and amplitude of the action potential are determined by the concentration of sodium in the external medium (e.g. Hodgkin & Katz, 1949*a*; Huxley & Stämpfli, 1951). Both groups of experiments are consistent with the theory that nervous conduction depends on a specific increase in permeability which allows sodium ions to move from the more concentrated solution outside a nerve fibre to the more dilute solution inside it. This movement of charge makes the inside of the fibre positive and provides a satisfactory explanation for the rising phase of the spike. Repolarization during the falling phase probably depends on an outflow of potassium ions and may be accelerated by a process which increases the potassium permeability after the action potential has reached its crest (Hodgkin, Huxley & Katz, 1949).

Outline of experiments

The general aim of this series of papers is to determine the laws which govern movements of ions during electrical activity. The experimental method was based on that of Cole (1949) and Marmont (1949), and consisted in measuring the flow of current through a definite area of the membrane of a giant axon from *Loligo*, when the membrane potential was kept uniform over this area and was changed in a stepwise manner by a feed-back amplifier. Two internal electrodes consisting of fine silver wires were thrust down the axis of the fibre for a distance of about 30 mm. One of these electrodes recorded the membrane potential, and the feed-back amplifier regulated the current entering the other electrode in such a way as to change the membrane potential suddenly and

hold it at the new level. Under these conditions it was found that the membrane current consisted of a nearly instantaneous surge of capacity current, associated with the sudden change of potential, and an ionic current during the period of maintained potential. The ionic current could be resolved into a transient component associated with movement of sodium ions, and a prolonged phase of 'potassium current'. Both currents varied with the permeability of the membrane to sodium or potassium and with the electrical and osmotic driving force. They could be distinguished by studying the effect of changing the concentration of sodium in the external medium.

The first paper of this series deals with the experimental method and with the behaviour of the membrane in a normal ionic environment. The second (Hodgkin & Huxley, 1952*a*) is concerned with the effect of changes in sodium concentration and with a resolution of the ionic current into sodium and potassium currents. Permeability to these ions may conveniently be expressed in units of ionic conductance. The third paper (Hodgkin & Huxley, 1952*b*) describes the effect of sudden changes in potential on the time course of the ionic conductances, while the fourth (Hodgkin & Huxley, 1952*c*) deals with the inactivation process which reduces sodium permeability during the falling phase of the spike. The fifth paper (Hodgkin & Huxley, 1952*d*) concludes the series and shows that the form and velocity of the action potential may be calculated from the results described previously.

A report of preliminary experiments of the type described here was given at the symposium on electrophysiology in Paris (Hodgkin *et al.* 1949).

Nomenclature

In this series of papers we shall regard the resting potential as a positive quantity and the action potential as a negative variation. V is used to denote displacements of the membrane potential from its resting value. Thus

$$V = E - E_r,$$

where E is the absolute value of the membrane potential and E_r is the absolute value of the resting potential, with signs taken in the sense outside potential minus inside potential. With this choice of signs it is logical to take $+I$ for inward current density through the membrane. These definitions make membrane current positive under an external anode and agree with the accepted use of the terms negative and positive after-potential. They conflict with the common practice of showing action potentials as an upward deflexion and are inconvenient in experiments in which an internal electrode measures potentials with respect to an external earth. Lower-case symbols (v_n) are employed when it is necessary to give potentials with respect to earth, but no confusion should arise since this usage is confined to the sections dealing with the experimental method.

Theory

Although the results described in this paper do not depend on any particular assumption about the electrical properties of the surface membrane, it may be helpful to begin by stating the theoretical assumption which determined the design and analysis of the experiments. This is that the membrane current may be divided into a capacity current which involves a change in ion density at the outer and inner surfaces of the membrane, and an ionic current which depends on the movement of charged particles through the membrane. Equation 1 applies to such a system, provided that the behaviour of the membrane capacity is reasonably close to that of a perfect condenser:

$$I = C_M \frac{\partial V}{\partial t} + I_i, \tag{1}$$

where I is the total current density through the membrane, I_i is the ionic current density, C_M is the membrane capacity per unit area, and t is time. In most of our experiments $\partial V/\partial t = 0$, so that the ionic current can be obtained directly from the experimental records. This is the most obvious reason for using electronic feed-back to keep the membrane potential constant. Other advantages will appear as the experimental results are described.

EXPERIMENTAL METHOD

The essential features of the electrode system are illustrated by Fig. 1. Two long silver wires, each 20 μ. in diameter, were thrust down the axis of a giant axon for a distance of 20–30 mm. The greater part of these wires was insulated but the terminal portions were exposed in the manner shown in Fig. 1. The axon was surrounded by a 'guard ring' system which contained the external electrodes. Current was applied between the current wire (*a*) and an earth (*e*), while the potential difference across the membrane could be recorded from the voltage wire (*b*) and an external electrode (*c*). The advantage of using two wires inside the nerve is that polarization of the current wire does not affect the potential recorded by the voltage wire. The current wire was exposed for a length which corresponded to the total height of the guard-system, while the voltage wire was exposed only for the height of the central channel. The guard system ensured that the current crossing the membrane between the partitions A_2 and A_3 flowed down the channel C. This component of the current was determined by recording the potential difference between the external electrodes *c* and *d*.

Internal electrode assembly

In practice it would be difficult to introduce two silver wires into an axon without using some form of support. Another requirement is that the electrode must be compact, since previous experience showed that axons do not survive well unless the width of an internal electrode is less than 150 μ. (Hodgkin & Huxley, 1945). After numerous trials the design shown in Fig. 4 was adopted. The first operation in making such an electrode was to push a length of the voltage wire through a 70 μ. glass capillary and twist it round the capillary in a spiral which started at the tip and proceeded toward the shank of the capillary. The spiral was wound by rotating the shank of the capillary in a small chuck attached to a long screw. During this process the free end of the wire was pulled taut by a weight while the capillary was supported, against the pull of the wire, by a fine glass hook. A second hook controlled the angle at which the wire left the capillary. When sufficient wire had been wound it was attached to the capillary by application of shellac solution,

cut close to the capillary and insulated with shellac in the appropriate regions (Fig. 4). The next operation was to wind on the current wire, starting from the shank and proceeding to the tip. Correct spacing of current and voltage wires was maintained by making small adjustments in the position of the second glass hook. When the current wire had been wound to the tip it was attached to the capillary, cut short and insulated as before. The whole operation was carried out under a binocular microscope. Shellac was applied as an alcoholic solution and was dried and hardened

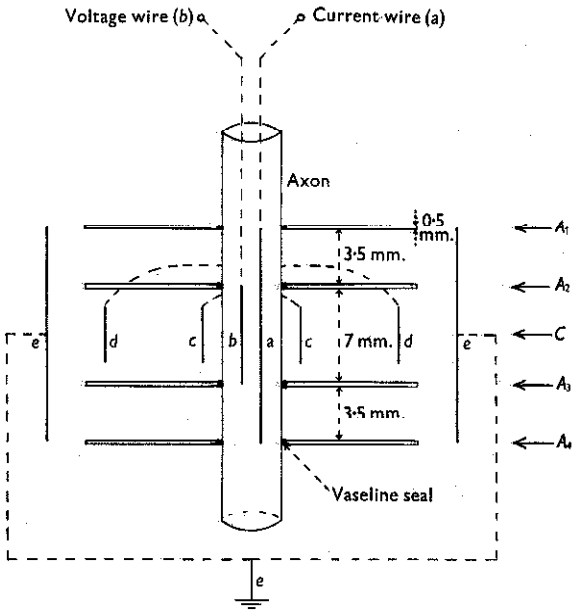

Fig. 1. Diagram illustrating arrangement of internal and external electrodes. A_1, A_2, A_3 and A_4 are Perspex partitions. *a*, *b*, *c*, *d* and *e* are electrodes. Insulated wires are shown by dotted lines. For sections through *A* and *C*, see Figs. 2 and 3.

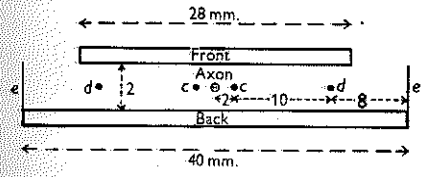

Fig. 2.

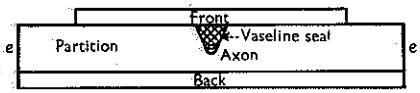

Fig. 3.

Fig. 2. Central channel of guard system. Section through *C*, Fig. 1. *c* and *d* are silver wires, *e* is a silver sheet. All dimensions are in mm.

Fig. 3. Partition of guard system. Section through A_1, A_2, A_3 or A_4, Fig. 1.

by baking for several hours under a lamp. Insulation between wires and across the shellac was tested so as to ensure that the film of shellac was complete and that the wires did not touch at any point. The exposed portion of the wires was then coated electrolytically with chloride. The electrode was first made an anode in order to deposit chloride and was then made a cathode in order to reduce some of the chloride and obtain a large surface of silver. This process was repeated a number of times ending with an application of current in the direction to deposit chloride. In this way an electrode of low polarization resistance was obtained.

In order to test the performance of the electrode it was immersed in salt solution and the current wire polarized by application of an electric current. In theory this should have caused no change in the potential difference between the voltage wire and the solution in which it was immersed. In practice we observed a very small change in potential which will be called 'mutual polarization'. Leakage between wires was a possible cause of this effect, but other explanations cannot be excluded.

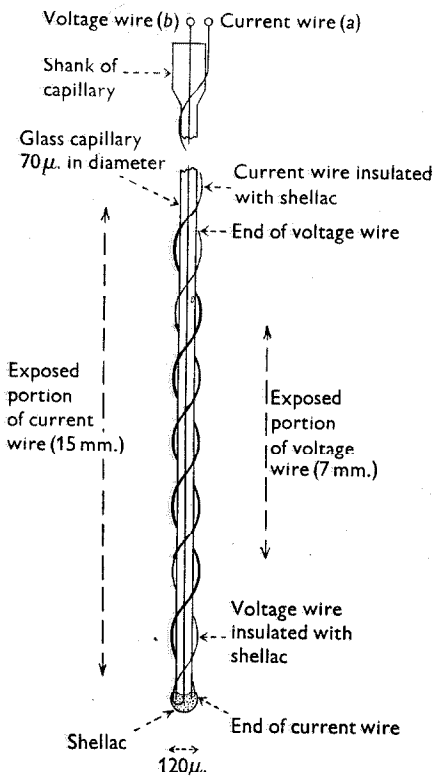

Fig. 4. Diagram of internal electrode (not to scale). The pitch of each spiral was 0·5 mm. The exposed portions of the wires are shown by heavy lines.

The general appearance of the electrode inside a giant axon is illustrated by Fig. 5. These photographs were obtained at an early stage of the investigation, and the axon was cleaned less carefully than in later experiments. The internal electrode differed from those finally employed in that both wires were wound from the shank of the electrode and that the pitch was somewhat greater.

Guard system

The general form of the guard system is shown in Figs. 1–3. It consisted of a flat box made out of Perspex which was divided into three compartments by two partitions A_2 and A_3 and closed with walls A_1 and A_4. The front of the box was removable and was made from a thin sheet of Perspex which could be sealed into position with vaseline. V-shaped notches were made in the two end walls and in the partitions. The partitions were greased and the notches filled with an oil-vaseline mixture in order to prevent leakage between compartments (Figs. 1 and 3). The guard ring assembly was mounted on a micromanipulator so that it could be manoeuvred into position after the electrode had been inserted. The outer electrode (e) was made from silver sheet while the

inner electrodes (*c*) and (*d*) were made from 0·5 mm. silver wire. Exposed portions of the electrodes were coated electrolytically with chloride and the wires connecting the electrodes with external terminals were insulated with shellac.

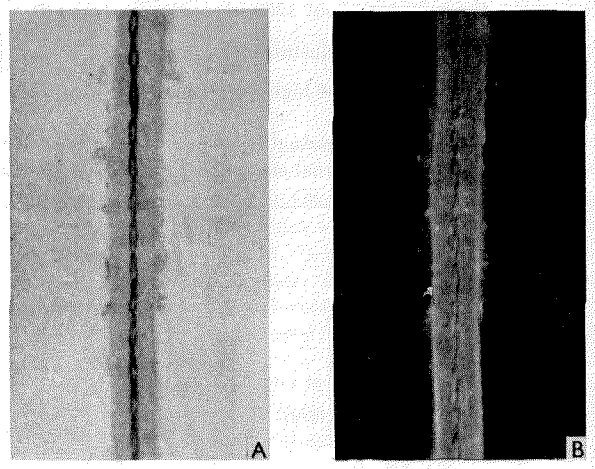

Fig. 5. Photomicrographs of giant axon and internal electrode. A, transmitted light; B, dark ground. The axon diameter was about 600 μ. The glass rod supporting the wires is not clearly seen.

Feed-back amplifier

A simplified diagram of the feed-back amplifier is shown in Fig. 6. It consisted of a differential d.c. amplifier with cathode follower input and output. The output of the amplifier was coupled to the input in such a way that negative feed-back was employed. This meant that any spontaneous change in membrane potential caused an output current to flow in a direction which restored the membrane potential to its original value. The level at which the potential was held constant was determined by the bias voltage v_3 and the control voltage v_4. v_3 was set so that no current passed through the nerve in the resting condition. This preliminary operation was carried out with the protective resistance R_f at its maximum value. This was important since an incorrect setting would otherwise have caused a large current to flow through the membrane. R_f was gradually reduced to zero; at the same time v_3 was adjusted to keep the membrane current zero. In order to change the membrane potential a rectangular pulse $\pm v_4$ was fed into the second stage of the amplifier. A large current then flowed into the membrane and changed its potential abruptly to a new level determined by

$$v_1 - v_2 = \beta v_4, \tag{2}$$

where v_1 and v_2 are the two input voltages and v_4 is the control voltage; β is a constant determined by resistance values and valve characteristics. Its value was of the order of 0·001. Any tendency to depart from Equation 2 was neutralized by a large output current which promptly restored the equilibrium condition defined by this relation.

In the majority of the experiments the slider of the potentiometer P was set to zero. Under these conditions the potential difference between the internal and external recording electrodes ($v_b - v_c$) was directly proportional to ($v_1 - v_2$). If α is the voltage gain of the cathode followers (about 0·9), then

$$v_b - v_c = \frac{2}{\alpha}(v_1 - v_2) = \frac{2\beta v_4}{\alpha}. \tag{3}$$

The performance of the feed-back amplifier was tested in each experiment by recording the time course of the potential difference between the internal and external electrodes. This showed that the recorded potential followed the control voltage with a time lag of about 1 μsec. and an

accuracy of 1–2%. It is therefore unnecessary to discuss the numerous approximations which have to be made in order to derive Equation 2.

The voltage gain of the feed-back amplifier and cathode followers was about 400 in the steady state. At high frequencies the gain was about 1200, since the condenser C_1 increased the gain under transient conditions. The mutual conductance of the feed-back system $\left[\frac{\partial i}{\partial (v_b - v_c)}\right]$ was about 1 mho in the steady state and 3 mhos at high frequencies. The maximum current that the amplifier could deliver was about 5 mA.

The method described would be entirely satisfactory if there were no resistance, apart from that of the membrane, between internal and external electrodes. In practice there was a small series

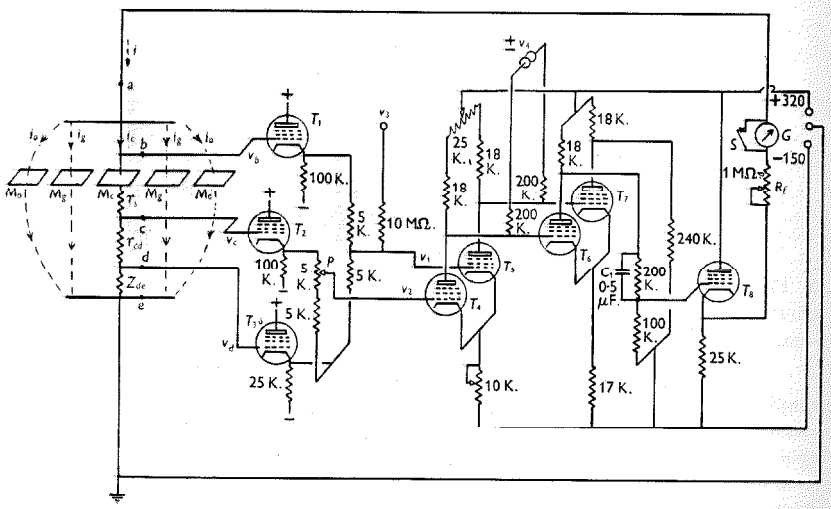

Fig. 6. Schematic diagram of feed-back amplifier. Screen resistances, grid stoppers and other minor circuit elements have been omitted. T_1, T_2, T_3 and T_8 are cathode followers; T_4, T_5, T_6 and T_7 are d.c. amplifiers. All valves were 6AK5 except T_1 and T_2 which were 1223. G is a microammeter used in setting-up. S is a switch for short-circuiting G. M_c is the membrane in the central section of the guard system. M_g, membrane in guard channels. M_o, membrane outside guard system. i_c, i_g and i_o are currents through these elements. r_{cd}, fluid-resistance used to measure current (74 Ω. at 20° C.). r_s, resistance in series with membrane (about 52 Ω. at 20° C.). z_{de}, impedance of large earthed electrode and sea water between d and e. Potentials are given with respect to earth.

resistance, represented by r_s in Fig. 6 and discussed further on p. 444. This meant that the true membrane potential was in error by the quantity $r_s i_c$. Thus

$$v_i - v_o = v_b - v_c - r_s i_c = 2\beta v_4/\alpha - r_s i_c, \tag{4}$$

where $v_i - v_o$ is the potential difference between the inner and outer surfaces of the membrane, r_s is the resistance in series with the membrane and i_c is the current flowing through the central area of membrane.

In principle the error introduced by r_s can be abolished by setting the potentiometer P to an appropriate value. All three cathode followers (T_1, T_2, T_3) had the same gain so that v_1 and v_2 were determined by the following equations:

$$v_1 = \tfrac{1}{2}\alpha\,(v_b + v_d), \tag{5}$$

$$v_2 = \tfrac{1}{2}\alpha\,[v_c + v_d + p\,(v_c - v_d)], \tag{6}$$

and

$$v_1 - v_2 = \tfrac{1}{2}\alpha\,[v_b - v_c - p\,(v_c - v_d)], \tag{7}$$

where p is proportional to the setting of the potentiometer P and varied between extremes of 0 and 1 and v_d is the potential of electrode d.

From Ohm's law

$$v_c - v_d = r_{cd} i_c, \tag{8}$$

where r_{cd} is the resistance of the central channel between electrodes c and d.

From Equations 4, 7 and 8

$$v_1 - v_2 = \tfrac{1}{2}\alpha [v_i - v_o + i_c (r_s - p r_{cd})]. \tag{9}$$

If $p = r_s/r_{cd}$

$$v_i - v_o = \frac{2}{\alpha}(v_1 - v_2) = \frac{2\beta v_4}{\alpha}. \tag{10}$$

The ratio r_s/r_{cd} was found to be about 0·7 and subsequent trials showed that a setting of $p = 0{\cdot}6$ could be used with safety. This procedure, which will be called compensated feed-back, was used successfully in seven of the later experiments. It had to be employed with considerable caution since a system of this type is liable to oscillate. Another difficulty is that if p is inadvertently made greater than r_s/r_{cd} the overall feed-back becomes positive and there is a strong probability that the membrane will be destroyed by the very large currents which the amplifier is capable of producing.

Auxiliary equipment

In addition to the feed-back amplifier we employed the following additional units: (1) A d.c. amplifier and cathode-ray oscillograph for recording membrane current and potential. (2) A voltage calibrator, with a built-in standard cell, giving ±110 mV. in steps of 1 mV. (3) A time calibrator consisting either of an electrically maintained 1 kcyc./sec. tuning fork, or a 4 kcyc./sec. fork with circuits to give pulses at 4, 2, 1 or 0·5 kcyc./sec. (4) Two units for producing rectangular pulses. These pulses were of variable amplitude (0–100 V.) and the circuits were arranged in such

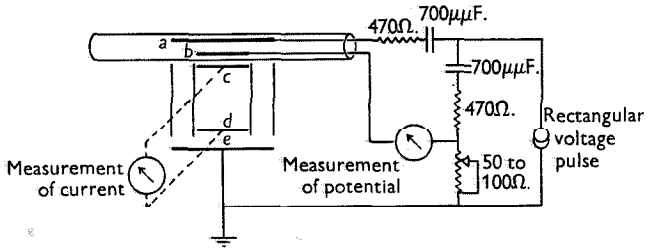

Fig. 7. Diagram of arrangement for recording response of membrane to short shock.

a way that the outputs of each generator were symmetrical with respect to earth. A single pulse generator was used in the early experiments, and its output was applied to the feed-back amplifier in the manner shown in Fig. 6. When required, the output of a second pulse generator was applied in parallel through a second pair of resistances. (5) An electrically operated refrigerator unit for cooling the preparation. All these items were of conventional design and need no detailed description.

Stimulation with brief currents

In the early stages of the work it was important to prove that the membrane was capable of giving an action potential of normal size. For this purpose we disconnected the feed-back amplifier and employed the arrangement shown in Fig. 7. A rectangular voltage step v_4 was applied to one internal electrode through a 700 μμF. condenser. The total area of membrane exposed to current flow from the electrode was about 0·3 cm.^{2} (1·5 cm. × π × 0·06 cm.). It therefore had a capacity of about 0·3 μF. When v_4 was suddenly changed by 10 V. the membrane potential was displaced by about 23 mV. (10 V. × 700/300,000). With this arrangement the membrane current consisted of very brief currents at the beginning and end of the voltage step. The size of the current could be varied by altering the size of the step, while the membrane current in the central channel of the guard-system could be measured by recording the potential difference

between electrodes *c* and *d*. The potential difference between the voltage wire (*b*) and the external electrode (*c*) was equal to the sum of the membrane potential and the potential difference across the ohmic resistance in series with the membrane. The second component was eliminated by the bridge circuit illustrated in Fig. 7.

Experimental procedure

Giant axons with a diameter of 400–800 μ. were obtained from the hindmost stellar nerve of *Loligo forbesi* and freed from all adherent tissue. Careful cleaning was important since the guard system did not operate satisfactorily if the axon was left with small nerve fibres attached to it. A further advantage in using cleaned axons was that the time required for equilibration in a test solution was greatly reduced by removing adherent tissue.

The axon was cannulated and mounted in the same type of cell as that described by Hodgkin & Huxley (1945) and Hodgkin & Katz (1949*a*). A conventional type of internal electrode, consisting of a long glass capillary, was thrust down the axon for a distance of 25–30 mm. This was then removed and the double wire electrode inserted in its place. Action potentials and resting potentials were recorded from the first electrode and the axon was rejected if these were not reasonably uniform over a distance of 20 mm. Another reason for starting with a conventional type of electrode was that the double wire electrode, in spite of the rigidity of its glass support, could not be inserted without buckling unless the axon had first been drilled with the glass capillary.

When the wire electrode was in position the guard system was brought into place by means of a micromanipulator. This operation was observed through a binocular microscope and care was taken to ensure that the central channel coincided exactly with the exposed portion of the internal voltage wire. The front of the guard-ring box was gently pressed into position and finally sealed by firm pressure with a pair of forceps. Before applying the front, spots of a vaseline-oil mixture were placed in such a position that they completed the seal round the axon when the front was pressed home (Figs. 1 and 3).

After the axon was sealed into position cold sea water (3–11° C.) was run into the cell and this temperature was maintained by means of a cooling coil which dipped into the cell. Air was bubbled through the cell in order to stir the contents and obtain a uniform temperature.

Before proceeding to study the behaviour of the axon under conditions of constant voltage its response to a short shock was observed. The experiment was discontinued if the action potential recorded in this way was less than about 85 mV. If the axon passed this test it was connected to the feed-back amplifier in the manner described previously.

Solutions were changed by running all the fluid from the cell and removing it from the guard-ring assembly with the aid of a curved capillary attached to a suction pump. A new solution was then run into the cell and was drawn into the guard rings by applying suction at appropriate places.

Calibration

The amplifier was calibrated at the end of each experiment, and all photographic records were analysed by projecting them on to a calibration grid. The readings obtained in this way were converted into current by dividing the potential difference between the two external electrodes *c* and *d* by the resistance between these electrodes (r_{cd}). This resistance was determined by blocking up the outer compartments of the guard-ring assembly and filling the central channel with sea water or with one of the standard test fluids. A silver wire was coated with silver chloride and inserted into the position normally occupied by the axon (Fig. 1). A known current was applied between the central wire and the outer electrode (*e*). The resistance between the two external electrodes *c* and *d* could then be obtained by measuring the change in potential difference resulting from a given application of current. It was found that the resistance between these electrodes was 74 Ω. when the central chamber was filled with sea water at 20° C. This value was close to that calculated from the dimensions of the system.

Membrane currents were converted to current densities by dividing them by the area of membrane exposed to current flow in the central compartment. The area was calculated from the measured axon diameter and the distance between the partitions A_2 and A_3 (Fig. 1).

RESULTS

Stimulation with brief currents

Before investigating the effect of a constant voltage it was important to establish that the membranes studied were capable of giving normal action potentials. This was done by applying a brief shock to one internal electrode and recording changes in membrane potential with the other. Details of the method are given on p. 431; typical results are shown in Fig. 8 (23° C.) and Fig. 9 (6° C.).

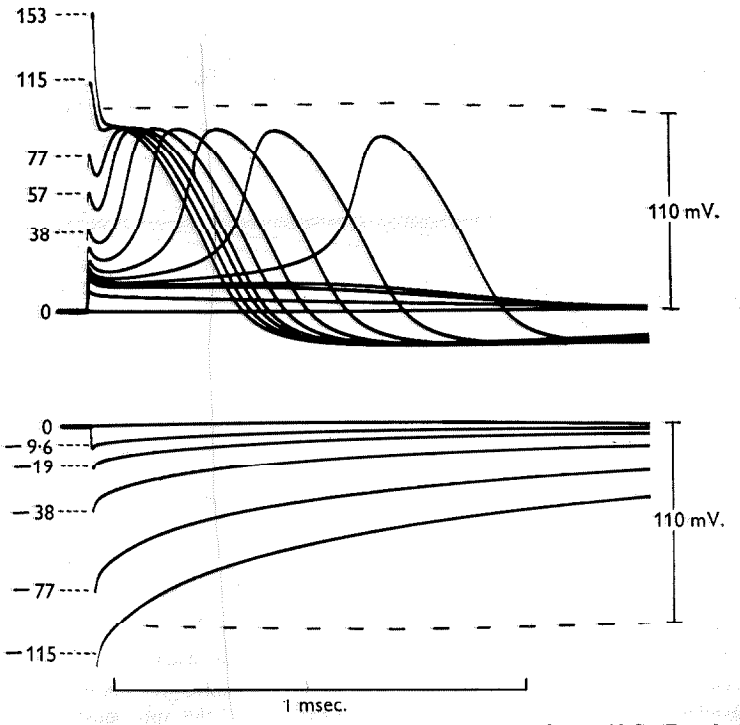

Fig. 8. Time course of membrane potential following a short shock at 23° C. Depolarizations shown upwards. Axon 18. The numbers attached to the curves give the strength of shock in mμcoulomb/cm.². Shock strengths for unlabelled curves are 29, 23, 19·2, 17·3, 16·7, 15·3, 9·6.

The shock used to displace the membrane potential was calibrated by recording the membrane current in the central channel (Fig. 7). This test showed that the current pulse consisted of a brief surge which was 95% complete in about 8 μsec. and reached a peak amplitude of about 50 mA./cm.² at the highest strengths. The total quantity of current passing through the central channel was evaluated by integrating the current record and was used to define the strength of the shock. The numbers attached to the records in Figs. 8 and 9 give the charge applied per unit area in mμcoulomb/cm.². It

will be seen that the initial displacement of membrane potential was proportional to the charge applied and that it corresponded to a membrane capacity of about 0·9 μF./cm.^{2}. Values obtained by this method are given in Table 1.

Although the initial charging process was linear, the subsequent behaviour of the membrane potential varied with the strength of shock in a characteristic

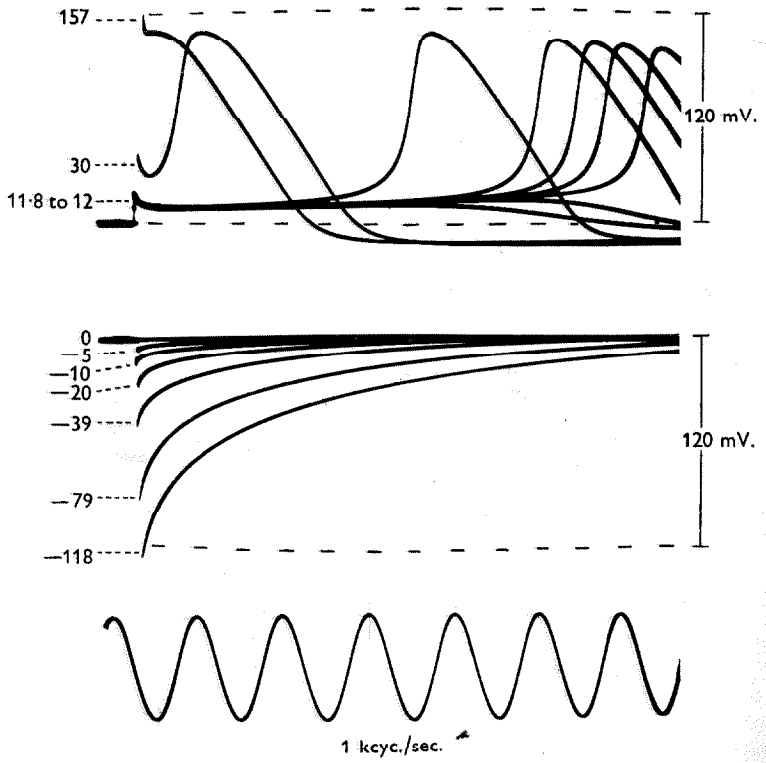

Fig. 9. Time course of membrane potential following a short shock at 6° C. Depolarization shown upwards. Axon 17. The numbers attached to the curves give the strength of shock in mμcoulomb/cm.^{2}. The initial displacement in the case of the uppermost curve cannot be seen; its value was about 200 mV.

manner. All the anodal records had the same general shape, but depolarizations of more than a few millivolts gave non-linear responses. If the depolarization was more than 15 mV. (Fig. 8) or 12 mV. (Fig. 9) the response became regenerative and produced an action potential of about 100 mV. If it was less than 12 or 15 mV. it was followed by a subthreshold response similar to that seen in most excitable tissues. If the potential was displaced to the threshold level it might remain in a state of unstable equilibrium for considerable periods of time. This is illustrated by Fig. 9 which shows the effect of a small variation of shock strength in the region of threshold.

Records such as those in Fig. 9 may be used to estimate the relation between membrane potential and ionic current. The total membrane current density (I) is negligible at times greater than 200 μsec. after application of the short

TABLE 1. Membrane capacities

Axon no.	Diameter (μ.)	Temperature (° C.)	Change in potential (mV.)	Membrane capacity (μF./cm.^{2}) Anodic	Cathodic	R_s (Ω.cm.^{2})	r_s (Ω.)	r_s/r_{cd}
			A. Voltage clamp					
13	520	9	+36 – 36	0·76	0·83	8·2	72	0·77
			+56 – 56	0·83	0·90			
			+98 – 98	0·83	0·96			
14	430	9	+36 – 34	0·81	0·83	5·8	61	0·65
17	588	7	+31 – 32	0·72	0·76	8·3	64	0·65
18	605	21	+30 – 31	0·92	0·91	5·5	41	0·57
19	515	8	+43 – 45	0·93	0·90	7·8	69	0·73
20	545	6	+42 – 43	0·88	0·86	9·1	76	0·77
21	533	9	+42 – 44	0·98	1·01	9·1	78	0·84
22	542	23	+40 – 41	1·01	1·03	4·0	34	0·50
25	603	8	+39 – 41	0·88	0·86	7·0	53	0·57
25*	603	7	+39 – 41	0·84*	0·82*	8·8*	66*	0·55*
26	675	20	+40 – 42	0·97	0·93	7·7	52	0·70
Average	—	—	—	0·88	0·90	7·3	60	0·68
				0·89				
			B. Short shock					
13	520	9	+58 – 50	1·07	1·11	—	—	—
17†	588	6	—	0·79†	0·74†	—	—	—
18†	605	23	—	0·85†	0·88†	—	—	—
Average	—	—	—	0·90	0·91	—	—	—
				0·91				
			C. Constant current					
29	540	21	—	—	1·49	6·4	42	0·57
41	585	4	—	—	0·78	11·9	92	0·88
Average	—	—	—	—	1·13	9·2	67	0·73
				1·13				
Average by all methods	—	—	—	0·91		7·6	61	0·68

* In this experiment choline was substituted for sodium in the external solution. The values obtained are excluded from the averages.

† In these experiments the shock strength was not measured directly but was obtained from the calibration for axon 13. The values for C_M are means obtained from a wide range of shock strengths.

shock. This means that the ionic current density (I_i) must be equal to the product of the membrane capacity per unit area (C_M) and the rate of depolarization. Thus if $I=0$, Equation 1 becomes

$$I_i = -C_M \frac{\partial V}{\partial t}. \tag{11}$$

Fig. 10 illustrates the relation between membrane potential and ionic current at a fixed time (290 μsec.) after application of the stimulus. It shows that

ionic current and membrane potential are related by a continuous curve which crosses the zero current axis at $V=0$, $V=-12$ mV. and $V=-110$ mV. Ionic current is inward over the regions -110 mV. $< V < -12$ mV. and $V>0$, and is outward for $V<-110$ mV. and -12 mV. $< V < 0$. $\partial I_i/\partial V$ is negative for -76 mV. $< V < -6$ mV. and is positive elsewhere.

A curve of this type can be used to describe most of the initial effects seen in Figs. 8 and 9. When the membrane potential is increased by anodal shocks the ionic current associated with the change in potential is in the inward direction. This means that the original membrane potential must be restored by an inward transfer of positive charge through the membrane. If the

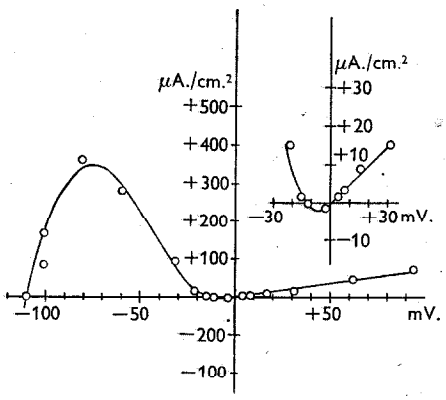

Fig. 10. Relation between ionic current density (I_i) and displacement of membrane potential (V). Abscissa: displacement of membrane potential from its resting value (anodal displacement shown positive). Ordinate: ionic current density obtained from $-C_M \frac{dV}{dt}$ (inward current shown positive). Inset: curve in region of origin drawn with tenfold increase in vertical scale. Axon 17; $C_M = 0{\cdot}74\,\mu$F./cm.^{2}; temperature 6·3° C. Measurements made 0·29 msec. after application of shock.

membrane potential is depolarized by less than 12 mV., ionic current is outward and again restores the resting condition by repolarizing the membrane capacity. At $V=-12$ mV., I_i is zero so that the membrane potential can remain in a state of unstable equilibrium. Between $V=-110$ mV. and $V=-12$ mV., I_i is inward so that the membrane continues to depolarize until it reaches $V=-110$ mV. If the initial depolarization is greater than 110 mV. I_i is outward which means that it will repolarize the membrane towards $V=-110$ mV. These effects are clearly seen in Figs. 8 and 9.

Membrane current under conditions of controlled potential

General description

The behaviour of the membrane under a 'voltage clamp' is illustrated by the pair of records in Fig. 11. These show the membrane current which flowed as a result of a sudden displacement of the potential from its resting value to

a new level at which it was held constant by electronic feed-back. In the upper record the membrane potential was increased by 65 mV.; in the lower record it was decreased by the same amount. The amplification was the same in both cases.

The first event in both records is a slight gap, caused by the surge of 'capacity current' which flowed when the membrane potential was altered suddenly. The surge was too rapid to be visible on these records, but was examined in other experiments in which low gain and high time base speed were employed (see p. 442). The ionic current during the period of constant potential was small when the membrane potential was displaced in the anodal direction, and is barely visible with the amplification used in Fig. 11. The top record in Fig. 12 gives the same current at higher amplification and shows

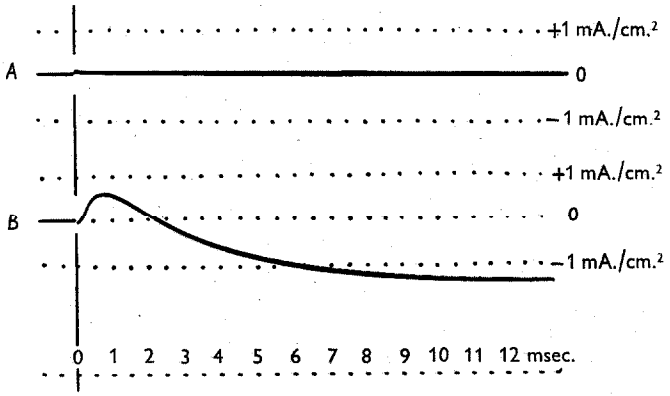

Fig. 11. Records of membrane current under a voltage clamp. At zero time the membrane potential was increased by 65 mV. (record *A*) or decreased by 65 mV. (record *B*); this level was then maintained constant throughout the record. Inward current is shown as an upward deflexion. Axon 41; diameter 585 μ. Temperature 3·8° C. Compensated feed-back.

that an increase of 65 mV. in the membrane potential was associated with an inward ionic current of about 30 μA./cm.^{2} which did not vary markedly with time. The sequence of events was entirely different when the membrane potential was reduced by 65 mV. (Fig. 11*B*). In this case the current changed sign during the course of the record and reached maximum amplitudes of $+600$ and $-1300\,\mu$A./cm.^{2}. The initial phase of ionic current was inward and was therefore in the opposite direction to that expected in a stable system. If it had not been drawn off by the feed-back amplifier it would have continued to depolarize the membrane at a rate given by Equation 11. In this experiment C_M was $0{\cdot}8\,\mu$F./cm.^{2} and I_i had a maximum value of $600\,\mu$A./cm.^{2}. The rate of depolarization in the absence of feed-back would therefore have been 750 V./sec., which is of the same general order as the maximum rate of rise of the spike (Hodgkin & Katz, 1949*a*, *b*). The phase of inward current was not maintained but changed fairly rapidly into a prolonged period of outward

current. In the absence of feed-back this current would have repolarized the membrane at a rate substantially greater than that observed during the falling phase of the spike. The outward current appeared to be maintained for an indefinite period if the membrane was not depolarized by more than 30 mV. With greater depolarization it declined slowly as a result of a polarization effect discussed on p. 445.

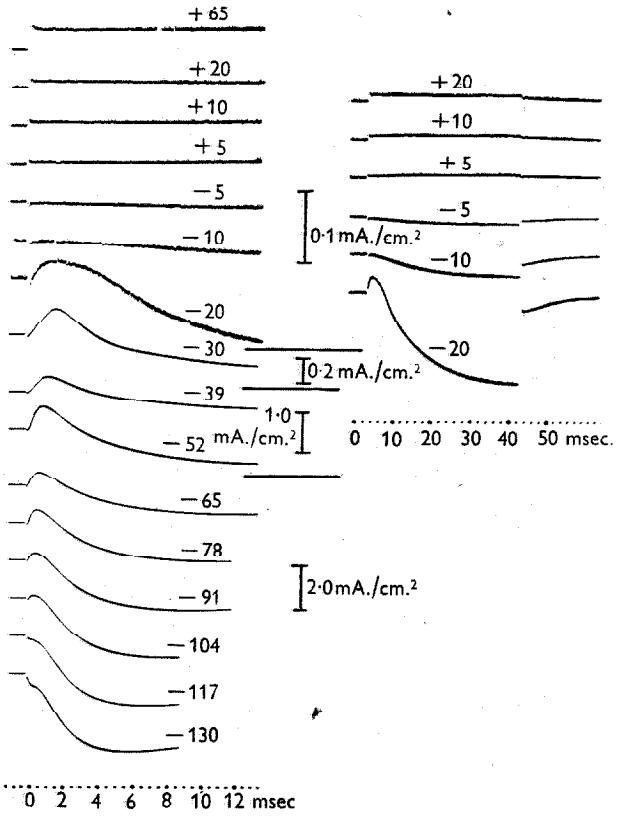

Fig. 12. Records of membrane current under a voltage clamp. The displacement of membrane potential (V) is given in millivolts by the number attached to each record. Inward current is shown as an upward deflexion. Six records at a lower time base speed are given in the right-hand column. Experimental details as in Fig. 11.

The features illustrated in Fig. 11 *B* were found over a wide range of voltages as may be seen from the complete family of curves in Fig. 12. An initial phase of inward current was conspicuous with depolarizations of 20–100 mV., while the delayed rise in outward current was present in all cathodal records. A convenient way of examining these curves is to plot ionic current density against membrane potential. This has been done in Fig. 13, in which the abscissa gives the displacement of membrane potential and the ordinate gives

the ionic current density at a short time (curve A) and in the 'steady state' (curve B). It will be seen that there is a continuous relation over the whole range, but that small changes in membrane potential are associated with large changes in current. At short times the relation between ionic current density

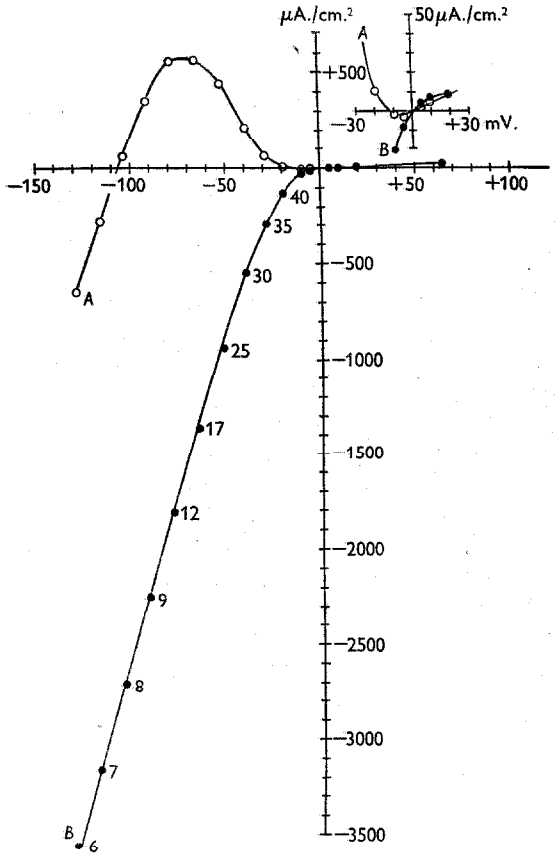

Fig. 13. Relation between membrane current density and membrane potential. Abscissa: displacement of membrane potential from its resting value in mV. Ordinate: membrane current density at 0·63 msec. after beginning of voltage step (curve A) and in 'steady state' (curve B). The numbers attached to curve B indicate the times in msec. at which the measurements were made. Inset: curves in region of origin drawn with a tenfold increase in the vertical scale. Inward current density is taken as positive and the membrane potential is given in the sense external potential minus the internal potential. Measurements were made from the records reproduced in Fig. 12 (3·8° C.).

and membrane potential is qualitatively similar to that obtained indirectly in Fig. 10. Ionic current is inward over the region -106 mV. $< V < -12$ mV. and for $V > 0$; it is outward for $V < -106$ mV. and for -12 mV. $< V < 0$. $\partial I_i/\partial V$ is negative for -70 mV. $< V < -7$ mV. and is positive elsewhere. More

quantitative comparisons are invalidated by the fact that the ionic current is a function of time as well as of membrane potential. At long times depolarization is invariably associated with an outward current and $\partial I_i/\partial V$ is always positive.

The electrical resistance of the membrane varied markedly with membrane potential. In Fig. 13, $\partial V/\partial I_i$ is about 2500 Ω.cm.^{2} for $V > 30$ mV. For $V = -110$ mV. it is 35 Ω.cm.^{2} (curve A) or 30 Ω.cm.^{2} (curve B). At $V = 0$, $\partial V/\partial I_i$ is 2300 Ω.cm.^{2} at short times and 650 Ω.cm.^{2} in the steady state. These results are comparable with those obtained by other methods (Cole & Curtis, 1939; Cole & Hodgkin, 1939).

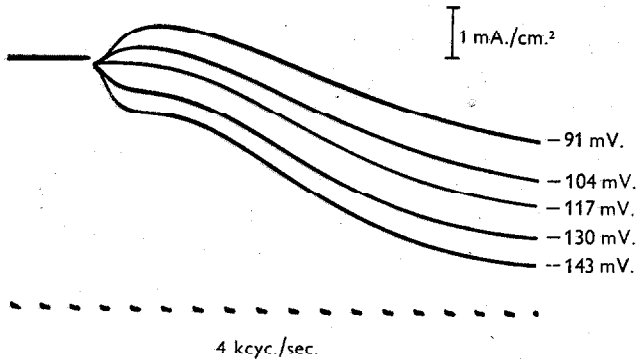

Fig. 14. Time course of membrane current during large depolarizations. Abscissa: time. Ordinate: inward current density. The numbers attached to the records give the displacement of membrane potential from its resting value. Axon 41; temperature 3·5° C. Compensated feed-back.

Fig. 14 illustrates the initial phase of ionic current at large depolarizations in greater detail. These records were obtained from the same axon as Fig. 12 but at an earlier stage of the experiment. They show that the initial 'hump' of ionic current changed sign at a potential of −117 mV. At −130 mV. the initial hump consists of outward current while it is plainly inward at −104 mV. The curve at −117 mV. satisfies the condition that $\partial I_i/\partial t = 0$ at short times and has no sign of the initial hump seen in the other records. It will be shown later that this potential probably corresponds to the equilibrium potential for sodium and that it varies with the concentration of sodium in the external medium (Hodgkin & Huxley, 1952*a*).

The effect of temperature

The influence of temperature on the ionic currents under a voltage clamp is illustrated by the records in Fig. 15. These were obtained from a pair of axons from the same squid. The first axon isolated was examined at 6° C. and gave the series of records shown in the left-hand column. About 5 hr. later the second axon, which had been kept at 5° C. in order to retard deterioration, was

examined in a similar manner at 22° C. Its physiological condition is likely to have been less normal than that of the first but the difference is not thought to be large since the two axons gave propagated action potentials of amplitude 107 and 103 mV. respectively, both measured at 22° C. The resting potentials were 55 mV. in both cases. The results obtained with the second axon are given in the right-hand column of Fig. 15. It will be seen that the general form and

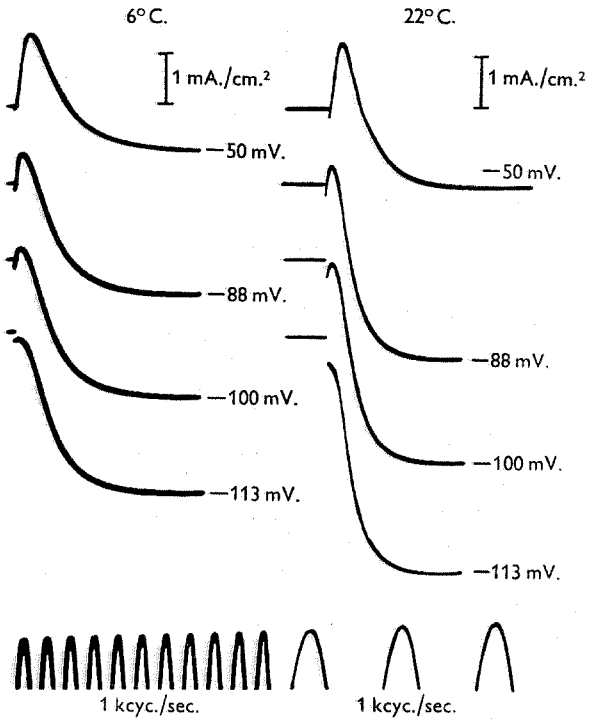

Fig. 15. Membrane currents at different temperatures. Axons 17 (6° C.) and 18 (22° C.), from the same squid. Inward current is shown as an upward deflexion. The numbers attached to each curve give the displacement of membrane potential. Uncompensated feed-back was employed.

amplitude of the two sets of records are similar but that the rate at which the ionic current changes with time was increased about sixfold by the rise in temperature of 16° C. It was found that the two families could be roughly superposed by assuming a Q_{10} of 3 for the rate at which ionic current changes with time. Values between 2·7 and 3·5 were found by analysing a number of experimental records obtained under similar conditions, but with different axons at different temperatures. In the absence of more precise information we shall use a temperature coefficient of 3 when it is necessary to compare rates measured at different temperatures.

The absolute magnitude of the current attained at any voltage probably varies with temperature, but much less than the time scale. In the experiment of Fig. 15 a rise of 16° C. increased the outward current about 1·5-fold, while the inward current at −50 mV. was approximately the same in the two records. Since the initial phase of inward current declined relatively rapidly as the axon deteriorated it is possible that a temperature coefficient of about 1·3 per 10° C. applies to both components of the current. Temperature coefficients of the order of 1·0–1·5 were also obtained by examining a number of results obtained with other axons.

The capacity current

The surge of current associated with the sudden change in membrane potential was examined by taking records at high time-base speed and low amplification. Tracings of a typical result are shown in Fig. 16. It will be seen

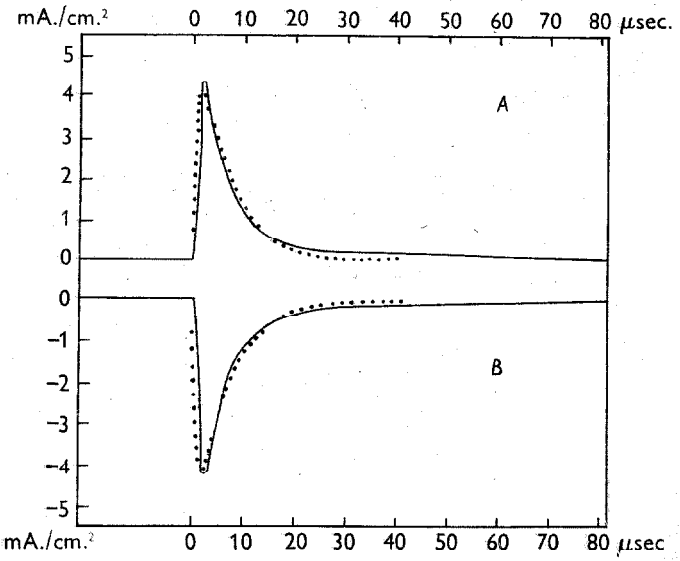

Fig. 16. Current through capacitative element of membrane during a voltage clamp. Abscissa: time in μsec. Ordinate: membrane current density (mA./cm.²) with inward current taken as positive. At $t=0$ the potential difference between external and internal electrodes was displaced +40 mV. in curve *A* or −40 mV. in curve *B*. The continuous curves were traced from experimental records. The dotted curves were calculated according to the equation

$$I^* = 6{\cdot}8\,[\exp(-0{\cdot}159t) - \exp(-t)],$$

where I^* is the current in mA./cm.² and t is time in μsec. This follows from the assumptions given in the text. Axon 25; temperature 8° C.

that the current records for anodal and cathodal changes are almost symmetrical and that the charging process is virtually complete in 50 μsec. In the anodal record the observed current declined from a peak of 4·5 mA./cm.² to a steady level of about 0·04 mA./cm.². The steady current is barely visible in the tracing

but could be seen more clearly at higher amplification and lower time-base speed; records taken under these conditions were similar to those in Fig. 12.

The membrane capacity was obtained from the change in potential and the area under the curves. A small correction was made for ionic current but the resting membrane conductance was sufficiently low for uncertainties here to be unimportant. In the experiment illustrated by Fig. 16*A* the charge entering the membrane capacity in 60 μsec. was 35 mμcoulomb/cm.^{2}, while the change in potential was 40 mV. Hence the membrane capacity per unit area was about 0·9 μF./cm.^{2}. Table 1 (p. 435) gives the results of other experiments of this kind. It also shows that replacement of all the sodium in sea water by choline had little effect on the membrane capacity and that there was no large change of capacity with temperature.

If a perfect condenser is short-circuited through zero resistance it loses its charge instantaneously. Fig. 16 suggests that the nerve capacity charged or discharged with a time constant of about 6 μsec. under a 'voltage clamp'. This raises the question whether the finite time of discharge was due to an imperfection in the membrane capacity or whether it arose from an imperfection in the method of holding the membrane potential constant. The records in Fig. 16 were obtained with uncompensated feed-back, which means that there was a small resistance in series with the capacitative element of the membrane. This clearly reduces the rate at which the membrane capacity can be discharged, and must be allowed for. It is also necessary to take account of the finite time constant of the recording amplifier (about 1 μsec. at this gain). Both effects have been considered in calculating the dotted lines in Fig. 16. These were drawn on the assumption that a 0·9 μF. condenser was charged to $\pm$40 mV. through a resistance of 7 Ω. and that the resulting pulses of current were recorded by an amplifier with an exponential time lag of 1 μsec. It will be seen that there is good agreement between the amplitude and general form of the two pairs of curves. Deviations at short times are not considered important since there was some uncertainty in the correction for amplifier delay.

At relatively long times ($>$ 25 μsec.) the current record shows a 'tail' which is not explained by the presence of a series resistance. This effect was present in all records and was larger at higher temperatures. It can be explained by supposing that the membrane capacity was not perfect but behaved in the manner described by Curtis & Cole (1938). The records in Fig. 16 are roughly consistent with a constant phase angle of 80°, while those at higher temperatures require somewhat lower values. These statements must be regarded as tentative since our experiments were not designed to measure the phase angle and do not give good data for quantitative analysis. For the time being the principal point to be emphasized is that the surge associated with a sudden

change in potential is adequately described by assuming that the membrane has a capacity of about 1 μF./cm.^{2} and a series resistance of about 7 Ω.cm.^{2}.

The surge of capacity current was larger in amplitude and occupied a shorter time when compensated feed-back was employed. These experiments were not suitable for analysis, since the charging current was oscillatory and could not be adequately recorded by the camera employed. All that could be seen in records of ionic current is a gap, as in Fig. 14.

Our values for the membrane capacity are in reasonable agreement with those obtained previously. Using transverse electrodes 5·6 mm. in length, Curtis & Cole (1938) obtained the following values in twenty-two experiments: average membrane capacity at 1 kcyc./sec., 1·1 μF./cm.^{2}, range 0·66 μF./cm.^{2} to 1·60 μF./cm.^{2}; average phase angle, 76°, range 64–85°.

The values for membrane capacity in the upper part of Table 1 were obtained by integrating the initial surge of current over a total time of about 50 μsec. If the phase angle is assumed to be 76° at all frequencies the average value of 0·89 μF./cm.^{2} obtained by this method is equivalent to one of 1·03 μF./cm.^{2} at 1 kcyc./sec. This is clearly in good agreement with the figures given by Curtis & Cole (1938), but is substantially less than the value of 1·8 μF./cm.^{2} mentioned in a later paper (Cole & Curtis, 1939). However, as Cole & Curtis point out, the second measurement is likely to be too large since the electrode length was only 0·57 mm. and no allowance was made for end-effects.

The series resistance

Between the internal and external electrodes there is a membrane with a resting resistance of about 1000 Ω.cm.^{2}. This resistance is shunted by a condenser with a capacity of about 1 μF./cm.^{2}. In series with the condenser, and presumably in series with the membrane as a whole, there is a small resistance which, in the experiment illustrated by Fig. 16, had an approximate value of 7 Ω.cm.^{2}. This 'series resistance' can be estimated without fitting the complete theoretical curve shown in that figure. A satisfactory approximation is to divide the time constant determining the decline of the capacitative curve by the measured value of the membrane capacity. This procedure was followed in calculating the values for the series resistance given in the upper part of Table 1. The symbol r_s gives the actual resistance in series with the central area of membrane, while R_s is the same quantity multiplied by the area of membrane exposed to current flow in the central channel of the guard system. The last column gives the ratio of r_s to the resistance (r_{cd}) between the current measuring electrodes, c and d. This ratio is of interest since it determined the potentiometer setting required to give fully compensated feed-back (pp. 430–1).

Another method of measuring the series resistance was to apply a rectangular pulse of current to the nerve and to record the potential difference (v_{bc}) between the internal electrode b and the external electrode c as a function of time. The current in the central channel of the guard system was also obtained by recording the potential difference (v_{cd}) between the external electrodes c and d. The two records were rounded to the same extent by amplifier delay so that the series resistance and the membrane capacity could be determined by fitting the record obtained from the internal electrode by the following equation

$$v_{bc} = \frac{r_s}{r_{cd}} v_{cd} + \frac{1}{r_{cd} C} \int_0^t v_{cd} \mathrm{d}t,$$

where c is the capacity of the area of membrane exposed to current flow in the central channel.

This analysis was made with two axons and gave satisfactory agreement between observed and calculated values of v_{bc}, with values of r_s/r_{cd} and C_M which were similar to those obtained by the voltage clamp method (see Table 1).

The observed value of the series resistance ($r_s = 61\,\Omega.$) cannot be explained solely by convergence of current between the electrodes used to measure membrane potential. Only about 30% was due to convergence of current between electrode *c* and the surface of the nerve, while convergence between the membrane and the internal electrode should not account for more than 25%, unless the specific resistance of axoplasm was much greater than that found by Cole & Hodgkin (1939). The axons used in the present work were surrounded by a dense layer of connective tissue, 5–20 μ. in thickness, which adheres tightly and cannot easily be removed by dissection. According to Bear, Schmitt & Young (1937) the inner layer of this sheath has special optical properties and may be lipoid in nature. It seems reasonable to suppose that one or other of these external sheaths may have sufficient resistance to account for 45% of the series resistance. There was, in fact, some evidence that the greater part of the series resistance was external to the main barrier to ionic movement. Substitution of choline sea water for normal sea water increased r_{cd} by 23%, but it reduced r_s/r_{cd} by only 3·5% (Table 1, axon 25). This suggests that about 80% of r_s varied directly with the specific resistance of the external medium. Since the composition of axoplasm probably does not change when choline is substituted for sodium (Keynes & Lewis, 1951) it seems likely that most of the series resistance is located outside the main barrier to ionic movement. Further experiments are needed to establish this point and also to determine whether the resistive layer has any measurable capacity.

Accuracy of method

The effect of the series resistance. The error introduced by the series resistance (r_s) was discussed on p. 430. Its magnitude was assessed by comparing records obtained with uncompensated feed-back ($p = 0$) with those obtained with compensated feed-back ($p = 0{\cdot}6$). The effect of compensation was most conspicuous with a depolarization of about 30 mV. Fig. 17 shows typical curves in this region. *A*, *B* and *C* were obtained with uncompensated feed-back; α, β and γ with compensated feed-back. *A* gives the potential difference between external and internal electrodes. *B* is the potential difference between the external electrodes used to measure current and is equal to the product of the membrane current and the resistance r_{cd}. The true membrane potential differs from *A* by the voltage drop across r_s which is equal to $(r_s/r_{cd})\,B$. *C* shows the membrane potential calculated on the assumption that r_s/r_{cd} had its average value of 0·68. α, β and γ were obtained in exactly the same manner as *A*, *B* and *C*, except that the potentiometer setting (p) was increased from 0 to 0·6. It will be seen that this altered the form of the upper record in a manner which compensates for the effect of current flow. The error in *C* is about 20%, while γ deviates by only about 2·5%. Hence any error present in β is likely to be increased eightfold in *B*. Since the two records are not grossly different, β may be taken as a reasonably faithful record of membrane current under a voltage clamp.

Experiments of this type indicated that use of uncompensated feed-back introduced errors but that it did not alter the general form of the current record. Since the method of compensated feed-back was liable to damage axons it was not employed in experiments in which the preparation had to be kept in good condition for long periods of time.

Polarization effects. The outward current associated with a large and prolonged reduction of membrane potential was not maintained, but declined slowly as a result of a 'polarization effect'. The beginning of this decline can be seen in the lower records in Fig. 12. It occurred under conditions which had little physiological significance, for an axon does not normally remain with a membrane potential of -100 mV. for more than 1 msec. Nor does the total current through the membrane approach that in Fig. 12.

In order to explain the effect it may be supposed either: (1) that 'mutual polarization' of the electrode (p. 428) is substantially greater inside the axon than in sea water; (2) that currents may cause appreciable changes in ionic concentration near the membrane; (3) that some structure in series with the membrane may undergo a slow polarization. We were unable to distinguish

between these suggestions, but it was clear that the 'polarization effect' had little to do with the active changes, since it was also present in moribund axons and was little affected by temperature.

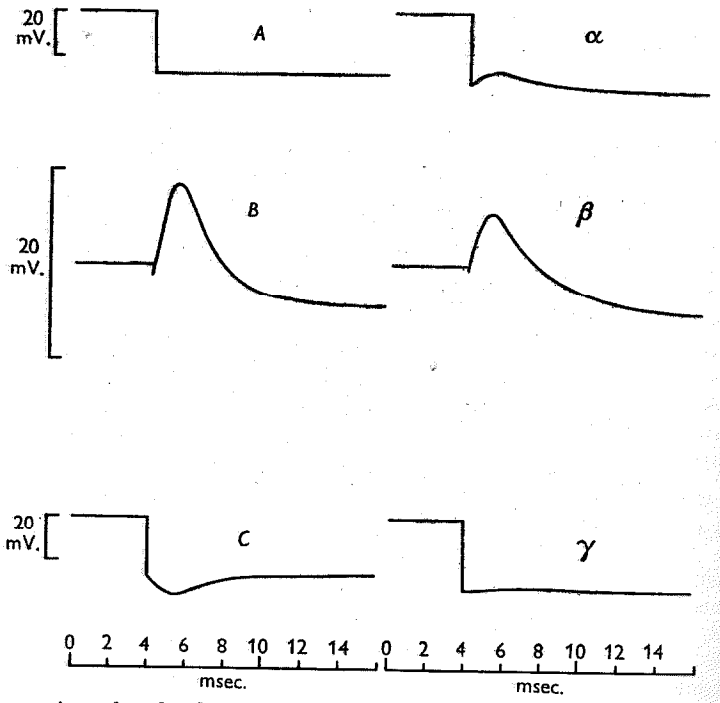

Fig. 17. Comparison of results obtained with uncompensated feed-back (A, B, C) and compensated feed-back (α, β, γ). A, α: potential difference between external and internal electrodes ($v_c - v_b$). B, β: potential difference between current measuring electrodes ($v_d - v_c$). C, γ: membrane potential calculated as $C = A - 0{\cdot}68B$, or $\gamma = \alpha - 0{\cdot}68\beta$. Records B and β may be converted into membrane current density by dividing by 11·9 Ω.cm.². Temperature 4° C. Axon 34.

SUMMARY

1. An experimental method for controlling membrane potential in the giant axon of *Loligo* is described. This depended on the use of an internal electrode consisting of two silver wires, a guard system for measuring membrane current and a 'feed-back' amplifier for clamping the membrane potential at any desired level.

2. Axons impaled with the double electrode gave 'all-or-nothing' action potentials of about 100 mV. when stimulated with a brief shock. The action potential had a well-defined threshold at a critical depolarization of about 15 mV. Depolarizations less than 10–15 mV. gave graded responses similar to those seen in other excitable tissues.

3. The feed-back amplifier was arranged to make the membrane potential undergo a sudden displacement to a new level at which it was held constant for

10–50 msec. Under these conditions the membrane current consisted of a brief surge of capacity current, associated with the sudden change in potential, and an ionic current during the period of maintained potential. The brief surge was proportional to the displacement of membrane potential and corresponded to the charging of a membrane with an average capacity of 0·9 μF./cm.^{2}. The sign and time course of the ionic current varied markedly with the membrane potential. *Anodal displacements gave small currents which were always* inward in direction. Depolarizations of less than 15 mV. gave outward currents which were small initially but increased markedly with time. Depolarizations of 15–110 mV. gave an initial phase of inward current which changed fairly rapidly into a large and prolonged outward current. The phase of inward current disappeared at about 110 mV. and was replaced by one of outward current. There was a continuous relation between ionic current and membrane potential. At short times this relation was similar to that derived from the rising phase of the action potential.

4. The maximum inward and outward ionic currents were little altered by temperature, but the rate at which the ionic current changed with time was *increased about threefold for a rise of* 10° C.

5. There was evidence of a small resistance in series with the capacitative element of the membrane. Errors introduced by this resistance were reduced by the use of compensated feed-back.

We wish to thank the Rockefeller Foundation for financial aid and the Director and staff of the Marine Biological Association for assistance at all stages of the experimental work.

REFERENCES

BEAR, R. S., SCHMITT, F. O. & YOUNG, J. Z. (1937). The sheath components of the giant nerve fibres of the squid. *Proc. Roy. Soc.* B, **123**, 496–529.

COLE, K. S. (1949). Dynamic electrical characteristics of the squid axon membrane. *Arch. Sci. physiol.* **3**, 253–258.

COLE, K. S. & CURTIS, H. J. (1939). Electric impedance of the squid giant axon during activity. *J. gen. Physiol.* **22**, 649–670.

COLE, K. S. & HODGKIN, A. L. (1939). Membrane and protoplasm resistance in the squid giant axon. *J. gen. Physiol.* **22**, 671–687.

CURTIS, H. J. & COLE, K. S. (1938). Transverse electric impedance of the squid giant axon. *J. gen. Physiol.* **21**, 757–765.

HODGKIN, A. L. & HUXLEY, A. F. (1945). Resting and action potentials in single nerve fibres. *J. Physiol.* **104**, 176–195.

HODGKIN, A. L. & HUXLEY, A. F. (1952*a*). Currents carried by sodium and potassium ions through the membrane of the giant axon of *Loligo*. *J. Physiol.* **116**, 449–472.

HODGKIN, A. L. & HUXLEY, A. F. (1952*b*). The components of membrane conductance in the giant axon of *Loligo*. *J. Physiol.* **116**, 473–496.

HODGKIN, A. L. & HUXLEY, A. F. (1952*c*). The dual effect of membrane potential on sodium conductance in the giant axon of *Loligo*. *J. Physiol.* **116**, 497–506.

HODGKIN, A. L. & HUXLEY, A. F. (1952*d*). A quantitative description of membrane current and its application to conduction and excitation in nerve. *J. Physiol.* (in the press).

HODGKIN, A. L., HUXLEY, A. F. & KATZ, B. (1949). Ionic currents underlying activity in the giant axon of the squid. *Arch. Sci. physiol.* **3**, 129–150.

HODGKIN, A. L. & KATZ, B. (1949*a*). The effect of sodium ions on the electrical activity of the giant axon of the squid. *J. Physiol.* **108**, 37–77.

HODGKIN, A. L. & KATZ, B. (1949*b*). The effect of temperature on the electrical activity of the giant axon of the squid. *J. Physiol.* **109**, 240–249.

HUXLEY, A. F. & STÄMPFLI, R. (1951). Effect of potassium and sodium on resting and action potentials of single myelinated nerve fibres. *J. Physiol.* **112**, 496–508.

KEYNES, R. D. & LEWIS, P. R. (1951). The sodium and potassium content of cephalod nerve fibres. *J. Physiol.* **114**, 151–182.

MARMONT, G. (1949). Studies on the axon membrane. *J. cell. comp. Physiol.* **34**, 351–382.

ROTHENBERG, M. A. (1950). Studies on permeability in relation to nerve function. II. Ionic movements across axonal membranes. *Biochim. biophys. acta*, **4**, 96–114.